Wavelength-Detuning Cross-Beam Energy Transfer Mitigation Scheme for Polar Direct Drive on SG-III

J. A. Marozas and E. M. Campbell

Laboratory for Laser Energetics, University of Rochester

Introduction

In direct-drive inertial confinement fusion (ICF), laser beams irradiate a plastic-coated shell of frozen deuterium–tritium (DT) and ablatively drive an implosion. The ultimate goal of ICF is ignition and energy gain; the minimum shell kinetic energy required for ignition (defined as when the energy from DT fusion reactions exceeds the laser energy incident on the target) is given by $E_{\min} \sim \alpha^{1.88} P_{\text{abl}}^{-0.77} v_{\text{imp}}^{-5.89}$ (Ref. 1), where the three parameters of the implosion—α, v_{imp}, and P_{abl} [adiabat (the ratio of the fuel pressure to the Fermi-degenerate pressure at peak implosion velocity), implosion velocity, and ablation pressure, respectively]—are determined primarily by the deposition of the laser energy into the coronal plasma of the target and heat conduction to the ablation surface. Cross-beam energy transfer (CBET)[2] has been identified in direct-drive experiments on the OMEGA[3] and National Ignition Facility (NIF)[4] lasers to reduce absorption, ablation pressure, and implosion velocity. The presence of CBET on the SG-III facility[5] is anticipated to cause similar issues by reducing target absorption and the resulting reduction in ablation pressure and implosion velocity.

CBET laser–plasma interaction results from two-beam energy exchange via stimulated Brillouin scattering,[2] which reduces absorbed light and consequently reduces ablation pressure and implosion velocity. The dominant CBET loss mechanism in direct drive occurs when rays counter-propagate (backscatter mode), increasing scattered light, as illustrated in Fig 1. For the ignition-relevant overlapped beam intensities of ~8×10^{14} W/cm^2 for NIF experiments, CBET is calculated to reduce laser absorption by 22%, the average implosion speed

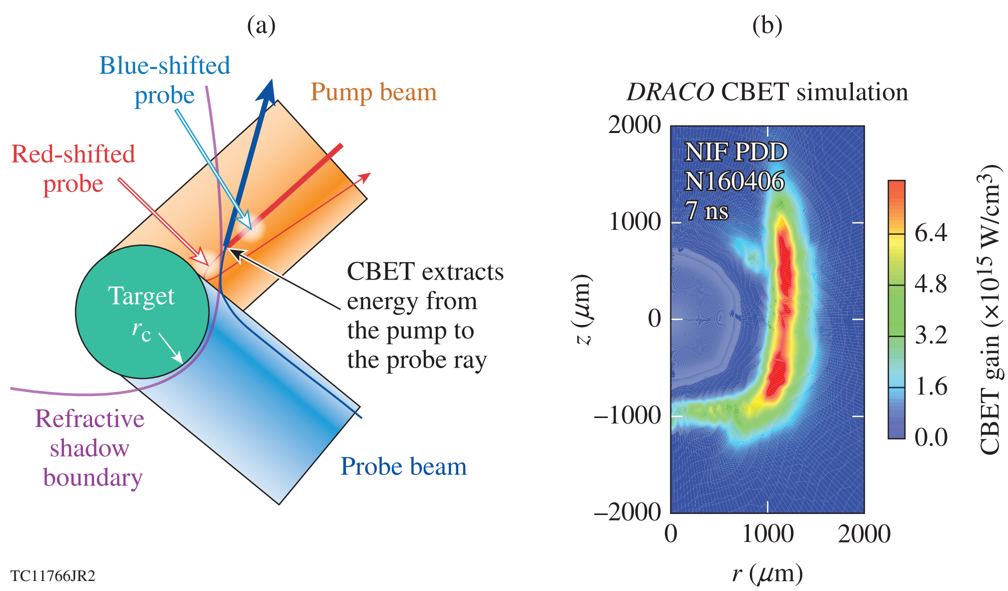

Figure 1
(a) The effect of cross-beam energy transfer (CBET) (backscatter mode) in polar direct drive (PDD) predominantly affects the equatorial region where rays interact. (b) The CBET effect dominates the equatorial region, as shown where successful CBET mitigation benefits the same region.

by ~9%, and the average ablation pressure by 35% (Ref. 6). These drive-related results are consistent with other ongoing OMEGA-[7] and NIF-scale[8] experiments. Reducing the target mass compensates for CBET losses, but the thinner shells become compromised as a result of hydrodynamic instability growth.[9] As shown by the above equation for E_{min}, efficient laser–energy coupling and hydrodynamic stability are essential aspects of direct-drive ICF, making CBET mitigation vital. Mitigation strategies of the deleterious CBET effects invoke combinations of spatial, temporal, and wavelength domains. Wavelength detuning works by altering the resonance condition between interacting beams.[2] Wavelength detuning was first examined for indirect drive[10] and subsequently for direct drive, but it was prematurely dismissed as a viable option.[11] Wavelength detuning was shown to mitigate CBET on the NIF in direct-drive experiments and to increase the drive relative to a no-detuning case;[6] *DRACO* simulations predict similar expectations on the SG-III facility.

Laser Facility and CBET Mitigation

The SG-III facility (see Fig. 2) has a similar indirect-drive configuration as the NIF, albeit with a single beam in each port as compared to NIF's quad architecture.[6,12] The SG-III facility provides a potential collaboration between LLE and SG-III. The indirect-drive beam geometry distributes the beam ports toward the poles of the target interaction chamber, forming cones of beams with a common polar angle.[13] This configuration must be altered to perform direct-drive experiments with a reasonably uniform drive. Repointing higher-intensity beams from lower latitudes toward the equator partially compensates for the indirect-drive port geometry and higher incident angles when illuminating direct-drive targets. In this modified configuration, referred to as polar direct drive (PDD),[14,15] CBET predictably dominates in the equatorial region,[6,12] where most of the cross-beam interactions occur, as shown in Fig. 1(b). As a result, PDD implosions tend to become oblate because CBET reduces the laser drive preferentially in the equatorial region. With this motivation, a basic wavelength-detuning strategy exploits the PDD configuration, where each hemisphere has a different wavelength or color. However, the nominal symmetric wavelength mapping on the NIF developed for indirect-drive targets precludes achieving hemispheric wavelength detuning using typical PDD repointing configurations.[15] A beam repointing method, called cone swapping,[12] was utilized on the NIF; it permits a partial hemispheric wavelength difference about the equator. The SG-III facility is assumed here to provide a more flexible color-to-beam mapping than available on the NIF. Cone swapping could still be applied to the SG-III facility if required but would produce nonoptimal results. For the purposes of this summary, the SG-III facility is assumed to provide three separate initial colors or wavelength shifts $\Delta\lambda_0 = \{\lambda_1, \lambda_2, \lambda_3\}$ detuned from a central wavelength $\lambda_0 \sim 351$ nm. The colors would be used to establish a bi- or tricolor distribution about the northern and southern hemispheres and yield the primary CBET mitigation strategy in any ICF direct-drive laser system.

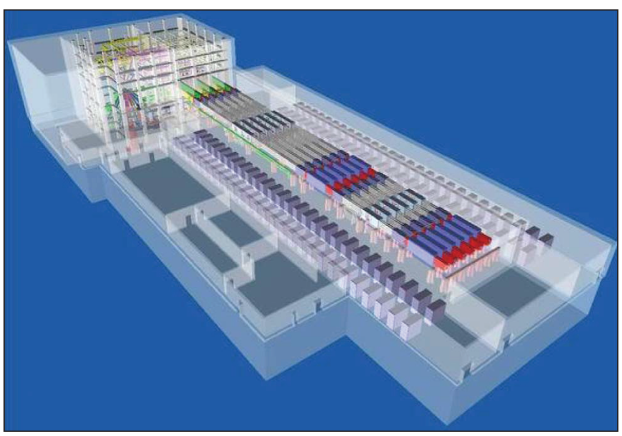

TC14723JR

Figure 2
The SG-III facility has a similar indirect-drive configuration as the NIF, albeit with single beams in each port as compared to NIF's quad architecture. The SG-III facility provides a potential collaboration between LLE and SG-III.

The far-field spot envelope [induced from distributed phase plates (DPP's)[16] and small-divergence smoothing] determines the overlapped nonuniformity on any direct-drive ICF laser system. For the PDD configuration, care is taken to design the spot shapes to account for necessary repointing of the beams toward the equator. An ideal PDD spot shape minimizes any energy that would otherwise be projected over the target horizon when repointed, while maintaining the best underlying beam profile using a method referred to as spot-masking apodization (SMA); this provides a substantial energy savings of ~15% to 20% (Ref. 17). In addition to the consideration of over-the-horizon energy loss, SMA can be employed as a CBET mitigation method by reducing the outer perimeter of the spot shape to a value that slightly underfills the full target diameter without severely effecting overlap nonuniformity like smaller spots.[12] Current SG-III spot shapes could be used in the interim (similar to experiments on the NIF[6]) before optimized DPP's are designed and manufactured.

Simulations Predictions

The initial proposed target designs for SG-III are an energy-scaled version of the first wavelength-detuning experiments performed on the NIF.[6] The warm plastic (CH) target is 640 μm in radius and has a 55-μm-thick CH shell filled with 20 atm of D_2 fuel at room temperature (see Fig. 3). A 100-kJ energy reference pulse provides the drive for the PDD target. This average pulse is a composite of different scaled energies for each ring of beams, where the different energies provide a nearly uniform drive that compensates for angular hydroefficiencies: the intensity on target near the equatorial region is larger than that near the polar region. The nonuniform delivered on-target intensity compensates for higher refraction suffered by equatorial rays as well as the lower hydrodynamic efficiency in that region. The pulse shape shown here would drive the target slowly (~300 μm/ns) to avoid large hydrodynamic instability growth seeded by laser imprint. Initial experiments would focus on the CBET mitigation properties and not initially on the fusion performance.

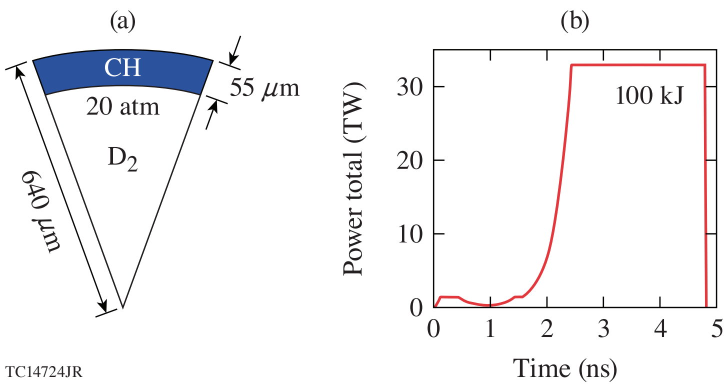

Figure 3
(a) The SG-III warm plastic (CH) target is 640 μm in radius and has a 55-μm-thick CH shell filled with 20 atm of D_2 fuel at room temperature. (b) The 100-kJ pulse provides a modest drive that could be enhanced after initial experiments.

The PDD repointing configuration suggested for the SG-III facility closely resembles what was recently shot on the NIF, where four rings of beams are distributed about the target surface (see Fig. 4). The PDD repointing configuration provides reasonable control of shock and shell uniformity during the implosion for the SG-III facility. The exact locations of the repointed spots can vary slightly for different target designs to optimize nonuniformity.

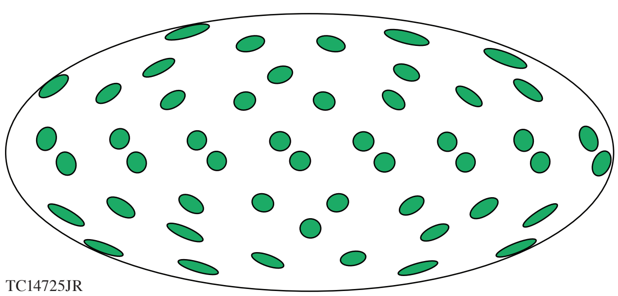

Figure 4
The suggested PDD repointing configuration provides reasonable control of shock and shell uniformity during the implosion for the SG-III facility, where four rings of beams are distributed about the target surface. Each green spot represents a beam port that has been repointed onto the initial target surface. The Hammer projection mapping is used.

Preliminary *DRACO*[12] simulations for the proposed PDD CBET mitigation experiments for the SG-III facility indicate promising results (see Fig. 5). These simulations show that reasonable uniformity can be achieved, assuming nonideal spot shapes that conform to those currently employed on the NIF. Simulations performed in the NIF's configuration using optimal DPP's have shown significant improvement in uniformity, which has boosted neutron yields by 2× to 3× in exploding-pusher configurations when compared to nonideal spot shapes.

Conclusion

The SG-III facility could provide a valuable platform to explore CBET mitigation in the PDD configuration in the 200-kJ energy range. CBET mitigation experiments would require some laser modifications to measure the mitigation efficacy such as

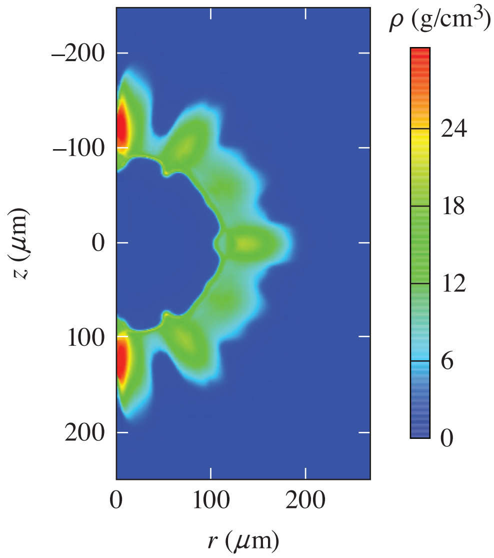

Figure 5
Initial *DRACO*[12] simulation results for PDD CBET mitigation experiments for the SG-III facility indicate promising results.

multiple tunable laser wavelengths, customized DPP's, and direct-drive target filling and manipulators. Higher shot repletion is expected, together with the ability to test a wide range of wavelength separation. The data that SG-III could provide would be valuable for future progress in direct-drive ICF.

This material is based upon work supported by the Department of Energy National Nuclear Security Administration under Award Number DE-NA0003856, the University of Rochester, and the New York State Energy Research and Development Authority.

1. M. C. Herrmann, M. Tabak, and J. D. Lindl, Nucl. Fusion **41**, 99 (2001).
2. C. J. Randall, J. R. Albritton, and J. J. Thomson, Phys. Fluids **24**, 1474 (1981).
3. T. R. Boehly *et al*., Opt. Commun. **133**, 495 (1997).
4. E. M. Campbell and W. J. Hogan, Plasma Phys. Control. Fusion **41**, B39 (1999).
5. W. Zheng *et al*., High Power Laser Sci. Eng. **4**, e21 (2016).)
6. J. A. Marozas *et al*., Phys. Rev. Lett. **120**, 085001 (2018).
7. P. B. Radha *et al*., J. Phys.: Conf. Ser. **688**, 012006 (2016).
8. M. Hohenberger *et al*., Phys. Plasmas **22**, 056308 (2015).
9. V. N. Goncharov *et al*., Phys. Plasmas **21**, 056315 (2014).
10. P. Michel *et al*., Phys. Plasmas **17**, 056305 (2010).
11. I. V. Igumenshchev *et al*., Phys. Plasmas **19**, 056314 (2012).
12. J. A. Marozas *et al*., Phys. Plasmas **25**, 056314 (2018).
13. M. L. Spaeth *et al*., Fusion Sci. Technol. **69**, 25 (2016).
14. S. Skupsky *et al*., Phys. Plasmas **11**, 2763 (2004).
15. J. A. Marozas *et al*., Phys. Plasmas **13**, 056311 (2006).
16. J. A. Marozas, J. Opt. Soc. Am. A **24**, 74 (2007).
17. J. A. Marozas *et al*., J. Phys.: Conf. Ser. **717**, 012107 (2016).